MNRAS **000**, 1–5 (2022) Preprint 22 April 2022 Compiled using MNRAS LATEX style file v3.0

Distant trans-Neptunian object candidates from NASA's *TESS* mission scrutinized: fainter than predicted or false positives?⋆

C. de la Fuente Marcos,[1]† R. de la Fuente Marcos,[2] O. Vaduvescu[3,4,5] and M. Stănescu[6]
[1]*Universidad Complutense de Madrid, Ciudad Universitaria, E-28040 Madrid, Spain*
[2]*AEGORA Research Group, Facultad de Ciencias Matemáticas, Universidad Complutense de Madrid, Ciudad Universitaria, E-28040 Madrid, Spain*
[3]*Isaac Newton Group (ING), Apt. de correos 321, E-38700, Santa Cruz de La Palma, Canary Islands, Spain*
[4]*Instituto de Astrofísica de Canarias (IAC), C/ Vía Láctea s/n, E-38205 La Laguna, Tenerife, Spain*
[5]*University of Craiova, Str. A. I. Cuza nr. 13, 200585, Craiova, Romania*
[6]*Bucharest Astroclub, Str. Cutitul de Argint 5, sector 4, 052034,Bucharest, Romania*

Accepted 2022 April 5. Received 2022 March 27; in original form 2022 March 6

ABSTRACT
NASA's *Transiting Exoplanet Survey Satellite* (*TESS*) is performing a homogeneous survey of the sky from space in search of transiting exoplanets. The collected data are also being used for detecting passing Solar system objects, including 17 new outer Solar system body candidates located at geocentric distances in the range 80–200 au, that need follow-up observations with ground-based telescope resources for confirmation. Here, we present results of a proof-of-concept mini-survey aimed at recovering two of these candidates that was carried out with the 4.2-m *William Herschel* Telescope and a QHY600L CMOS camera mounted at its prime focus. For each candidate attempted, we surveyed a square of over 1°×1° around its expected coordinates in Sloan r'. The same patch of sky was revisited in five consecutive or nearly consecutive nights, reaching S/N>4 at r'<23 mag. We focused on the areas of sky around the circumpolar *TESS* candidates located at (07^{h}:00^{m}:15^{s}, +86°:55′:19″), 202.8 au from Earth, and (06^{h}:39^{m}:47^{s}, +83°:43′:54″) at 162.1 au, but we could not recover either of them at $r' \leqslant 23$ mag. Based on the detailed analysis of the acquired images, we confirm that either both candidates are much fainter than predicted or that they are false positives.

Key words: methods: observational – techniques: photometric – Kuiper belt: general – minor planets, asteroids: general – Oort Cloud – planets and satellites: detection.

1 INTRODUCTION

Our degree of understanding of the structure of the Solar system beyond the trans-Neptunian or Kuiper belt and out into the Oort cloud remains very limited. The discoveries of 2018 VG_{18}, found at a heliocentric distance of about 123 au with unfiltered magnitude 24.6 (Sheppard et al. 2018), and 2018 AG_{37}, found at 132 au with G=25.3 mag (Sheppard, Tholen & Trujillo 2021), represent the opening of a new window into this remote region, the Solar system beyond 100 au from the Sun. Although just two objects have been detected with current distances >100 au, they are both following highly eccentric orbits and are arguably similar (in terms of their orbital properties) to several other confirmed Centaurs and scattered disc objects.

NASA's *Transiting Exoplanet Survey Satellite* (*TESS*)[1] is performing a homogeneous survey of the sky from space in search of transiting exoplanets (Ricker et al. 2015) —since 2018 it has observed approximately 80 per cent of the sky— but it is also capable of detecting passing Solar system small bodies (see e.g. Pál, Molnár & Kiss 2018; Holman, Payne & Pál 2019; McNeill et al. 2019; Payne, Holman & Pál 2019; Pál et al. 2020; Woods et al. 2021). By shift-stacking *TESS* images, Rice & Laughlin (2020) were able to recover three previously known outer Solar system bodies: 90377 Sedna (2003 VB_{12}) at about 84 au from the Sun with V=20.64 mag, 2015 BP_{519} at about 54 au with V=21.81 mag, and 523622 (2007 TG_{422}) at about 37 au with V=22.32 mag. Rice & Laughlin (2020) then applied a blind search shift-stacking algorithm to *TESS* sectors 18 and 19, and singled out 17 new outer Solar system body candidates, which need to be followed up with ground-based observations for confirmation. Their technique combines (stacks) a series of images, acquired at different times, to turn an undetected source into a brighter, single point-like occurrence. The stacking is done along different paths (shifts), assuming that the optimal one leads to the highest S/N for the newly detected source.

The *TESS* candidate objects are located at geocentric distances

⋆ Based on service observations (proposals SW2021a24 and SW2021a10) made with the 4.2-m *William Herschel* Telescope (*WHT*), operated by the *Isaac Newton* Group at the Observatorio del Roque de los Muchachos, La Palma, Spain, of the Instituto de Astrofísica de Canarias.
† E-mail: nbplanet@ucm.es
[1] https://heasarc.gsfc.nasa.gov/docs/tess/primary.html

in the range 80–200 au; the list of candidates in table 2 of Rice & Laughlin (2020) includes eight objects located farther than 100 au from the Sun (referred to epochs 2458838.92 JD or 10:4:48.00 UT on December 21, 2019 and 2458810.25 JD or 18:0:0.00 UT on November 22, 2019) that, if confirmed, would join 2018 VG_{18} and 2018 AG_{37} as the farthest Solar system objects ever observed. Confirming the existence of any of these eight distant candidates can significantly increase our knowledge of the outer Solar system as proper orbit determinations (the published data give only their instantaneous positions over two years ago) may enable their eventual physical and dynamical characterization (see e.g. de León, de la Fuente Marcos & de la Fuente Marcos 2017). Furthermore, the study of additional distant trans-Neptunian objects (TNOs) may help in confirming or rejecting the presence of putative planetary bodies beyond the trans-Neptunian belt (see e.g. de la Fuente Marcos & de la Fuente Marcos 2014; Trujillo & Sheppard 2014; Batygin & Brown 2016).

In this Letter, we present results of a proof-of-concept mini-survey carried out with the 4.2-m *William Herschel* Telescope (*WHT*)[2] and a QHY600L CMOS camera mounted temporarily on-axis at the prime focus of the *WHT* (PF-QHY)[3]. The survey was aimed at recovering two of the most distant new outer Solar system body candidates found in data from NASA's *TESS* mission and discussed by Rice & Laughlin (2020). In Section 2, we describe the observations acquired and in Section 3, we present the results of our analyses. A discussion is presented in Section 4. Finally, our conclusions are summarized in Section 5.

2 OBSERVATIONS

We obtained Sloan r' CMOS images of two fields — the first one in Cepheus and the second one in Camelopardalis (see Fig. 1) — as squares of over 1°×1° with *WHT* on July 2, 3, 4, 6, and 8, 2021. The QHY camera (model QHY600L)[4] used in this proof-of-concept mini-survey is based on a back-illuminated CMOS detector (Sony IMX455)[5], with 9576×6388 3.8-μm pixels, giving a field of view of 10.′7×7.′1 with a scale of 0.″067 pixel^{-1} at the prime focus of the *WHT*; with the recommended binning of 4×4 that was used in our study, the scale became 0.″267 pixel^{-1}. The camera was tilted by 90° so the longest dimension of the CMOS chip would be along the right ascension axis, optimizing the scanning process in terms of time used on-sky.

Each square patch of sky was densely sampled with 77 pointings — each one of 10.′7×7.′1 and with sufficient overlapping between neighbouring pointings (see Fig. 1). The 77 pointings of both square patches were repeated five nights (see Table 1). The pointings were carried out using a Python (Van Rossum and Drake 1995) script, scanning the patch of sky of slightly over one square degree after reading the coordinates of the centre of the field as input. Each individual pointing had an exposure time of 30 s with sidereal tracking. This choice should produce detections with S/N>4 at Sloan r'<23 mag in good seeing (⩽1.″2, see the discussion in Section 4). Due to the circumpolar nature of the target fields, they were observed at low elevations in the range 20°–30° — airmasses in the range 2.21–2.27 for the field in Cepheus and 2.52–2.61 for the one in Camelopardalis. The target candidates move at a rate of the order of 1″ h^{-1}; therefore, if a target field is revisited within 24 h, it should be relatively straightforward to identify the moving objects (if they are present in the imaged fields) by visually blinking the images for example. In our case, detections were flagged via software and subsequently validated or rejected after human analysis.

Table 1. Observations from *WHT*. Information includes date, Julian date, time used on-sky, *WHT* seeing range (Differential Image Motion Monitor, DIMM, values), and dark time window during the night. The images were all acquired during dark time.

Date (2021)	Julian date	UT-range (h:m) UT	seeing (″)	Dark time (h:m) UT
July 2	2459398	22:40 – 00:45	0.8 – 1.3	21:48 – 1:43
July 3	2459399	21:45 – 23:55	0.6 – 1.1	21:48 – 2:13
July 4	2459400	21:38 – 00:24	0.6 – 1.2	21:47 – 4:45
July 6	2459402	22:43 – 00:50	0.6 – 0.9	21:47 – 4:46
July 8	2459404	02:30 – 04:30	1.0 – 2.0	21:47 – 4:47

The data were processed by the automatic pipelines of the Umbrella suite (Stănescu & Văduvescu 2021), with human-validated detections. The processing of the raw frames into detection-ready images was carried out with the Umbrella IPP (Image pre-Processing Pipeline) that is a new component, not described in the original Umbrella paper. This new component uses dark and flat processing built on top of Umbrella2 (Stănescu 2020) and plate solving and field correction through AstrOmatic (Bertin & Arnouts 1996; Bertin et al. 2002; Bertin 2006). Dark images were used to remove any hot pixels. The detection pipeline applied was the reference blink pipeline (with tweaks and improvements specifically designed for this survey) called through the Webrella component, a web-based front-end application that allowed the entire collaboration to have quick access to the pipeline output. All the processing was performed on the server of the EUROpean Near Earth Asteroids Research (EURONEAR)[6] project at the University of Craiova. In case of recovering a putative candidate, its nature could be confirmed statistically using e.g. the software discussed by Bernstein & Khushalani (2000).

3 RESULTS

The two fields observed correspond to those of candidates 9 and 11 in table 2 of Rice & Laughlin (2020). Candidate 9 is the farthest one in their list, it is located at a geocentric distance of 202.8 au towards (α, δ) = (105.°0573, +86.°9216) in Cepheus, and it has V=21.77 mag. Candidate 11 is the third farthest in Rice & Laughlin (2020) with a geocentric distance of 162.1 au and observed projected towards (99.°9219, +83.°7321) in Camelopardalis with V=21.92 mag. From the data in Rice & Laughlin (2020), the ecliptic latitude of candidate 9 is 63.°6 and that of candidate 11 is 60.°4; being both so distant, their orbital inclinations, i, must be significant and this fact adds another intriguing property to these candidates. The confirmed extreme TNO (ETNO) 2015 BP_{519} — also detected by Rice & Laughlin (2020) — is considered an outlier with i=54° (Becker et al. 2018; de la Fuente Marcos & de la Fuente

[2] https://www.ing.iac.es/astronomy/telescopes/wht/
[3] https://www.ing.iac.es//Astronomy/instruments/pf-qhy/
[4] https://www.qhyccd.com/qhy600m-c/
[5] https://www.sony-semicon.co.jp/products/common/pdf/IMX455AQK-K_Flyer.pdf
[6] http://www.euronear.org/

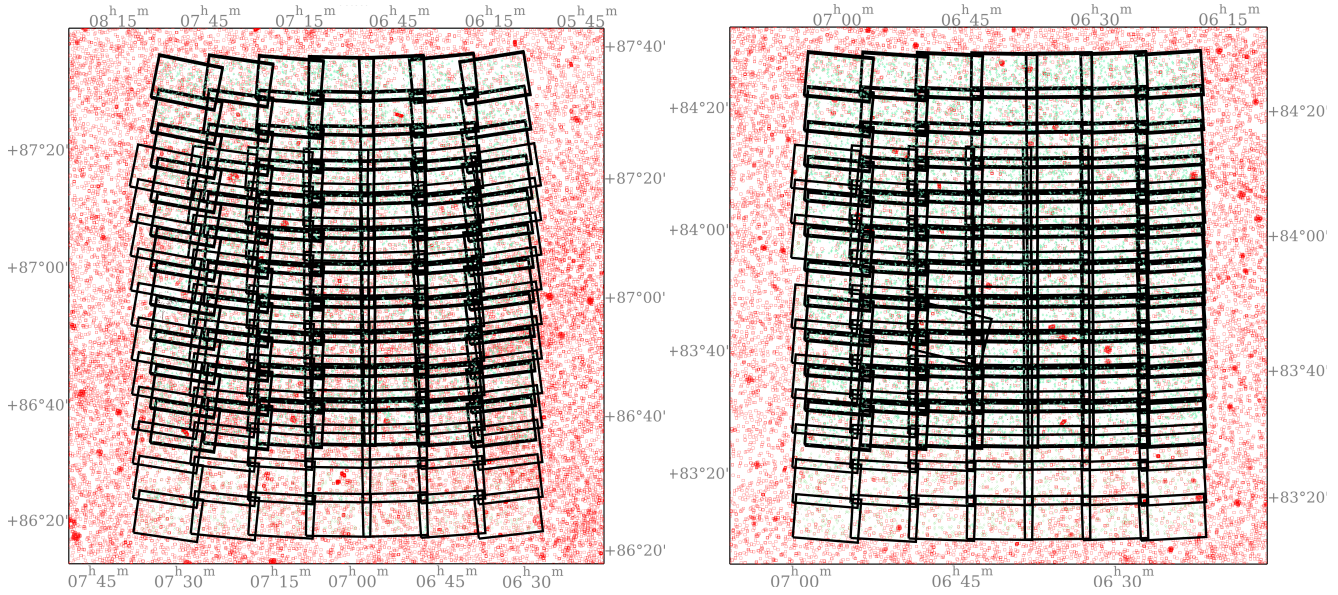

Figure 1. Fields observed by our survey. In both panels, North is up, East to the left. All the pointings (2 fields×77 pointings per field×5 nights per field) have been plotted. The left-hand side panel shows the field in Cepheus and centred towards (α, δ) = (105.°0573, +86.°9216), while the right-hand panel displays the field in Camelopardalis and centred towards (99.°9219, +83.°7321). The single, oddly rotated pointing was due to a short-lived technical issue and it does not affect our conclusions. Pointings for July 8 appear somewhat shifted due to another, different technical issue but this does not have an impact on our conclusions because data from the fifth night were only used as a redundant consistency check.

Marcos 2018) and it was observed at an ecliptic latitude close to −54° when discovered. In addition to being outliers in terms of orbital inclination, the candidates (if real) could be outliers in terms of size (assuming typical values for the albedo) as they would both be distant and comparatively bright within the context of the known TNO populations.

In addition to the Umbrella2-based automated detection pipeline, we used the Astrometrica[7] software (Raab 2012) in automated and visual blinking mode, as well as pure visual blinking with DS9[8] (Joye & Mandel 2003), to search for moving objects in both fields. Automated and visual analysis of the data collected did not produce any moving object detections. Querying the MPChecker[9] tool of the Minor Planet Center (MPC, Rudenko 2016; Hernandez, Hankey & Scott 2019)[10] revealed that no known small bodies could have been found projected towards the regions surveyed at the observed times. The high ecliptic latitude of the imaged fields precluded any detection of new members of the main asteroid belt and new members of the near-Earth object (NEO) populations were not expected to be detected due to the slow cadence of our survey. In addition to the targeted *TESS* candidates, our survey may only have detected relatively slow moving objects with high orbital inclination. No such objects emerged during the data analysis. Fitzsimmons (2000) pointed out that, when observing towards the ecliptic and a few tens of degrees from it, the apparent sky density of regular TNOs translates into one object brighter than R=23.0 mag per square degree of sky. Therefore, not finding any TNOs in over one square degree of sky at high ecliptic latitude is consistent with the expectations. The fields studied are seldom observed by surveys targeting the outer Solar system.

[7] http://www.astrometrica.at/
[8] https://sites.google.com/cfa.harvard.edu/saoimageds9
[9] https://minorplanetcenter.net/cgi-bin/checkmp.cgi
[10] https://minorplanetcenter.net

4 DISCUSSION

As pointed out above, we failed to recover candidates 9 and 11 identified by Rice & Laughlin (2020). In getting a null result, we must provide some indication of the sensitivity of our study. In a survey such as this one, the typical issues that would negatively impact sensitivity are: having an improper cadence, incorrect survey area size (perhaps too small), or insufficient depth. Here, we discuss these three sources of lack of sensitivity and their possible effects on our results. As shown in Table 1, the Moon could not possibly have been a factor in the non-detection of the candidates as the sky was dark during the time intervals used on-sky.

In our study, each field in the survey area was repeatedly revisited at variable cadence intervals. Each main field (one in Cepheus and one in Camelopardalis) was sampled with 77 pointings that took about one hour to be completed. Table 1 shows that the seeing was variable during the observations; however, the range of variability was 0.″6–1.″3 with the exception of the last night of the survey, July 8, when the spanning interval was (1″, 2″). In general and for each night and field, the quality of the images associated with the 77 pointings is reasonably homogeneous. Then, Table 1 shows that each main field was revisited with a cadence of 24 h (first three nights) or 48 h (last two nights). The rate of motion of a Solar system body located at a heliocentric distance s is maximum at opposition and minimum near quadrature. The actual values can be estimated under the circular and coplanar orbits approximation using (see e.g. Jewitt 1999; Fitzsimmons 2000):

$$\mu_{\rm opp} = \frac{3547.2}{s + \sqrt{s}} \quad \text{arcsec d}^{-1}\,, \tag{1}$$

$$\mu_{\rm qua} = \frac{3547.2}{s^{3/2}} \quad \text{arcsec d}^{-1}\,, \tag{2}$$

where 3547.2 is the mean orbital angular motion of our planet in arcseconds per day and s is measured in au. These approximations are good enough for objects observed near perihelion or aphelion

(as it could be the case for some *TESS* candidates); in a more general situation, the rate of motion considering a highly eccentric orbit might be a factor two slower than in the circular approximation. The impact of the inclination is rather negligible. For candidate 9, s∼200 au so $\mu_{\rm opp}$=16.″6 d^{-1} and $\mu_{\rm qua}$=1.″3 d^{-1}; for candidate 11 with s∼160 au, the respective values are 20.″5 d^{-1} and 1.″8 d^{-1}. As the seeing was mostly <1.″3 and the cadence was ⩾24 h, it is virtually impossible that the cadence intervals may have played any role in the non-detection of the candidates.

Our survey scanned square patches of sky of over 1°×1° (see Fig. 1) that may perhaps be not large enough to ensure that the candidates appear projected towards the region imaged. The only relevant data from Rice & Laughlin (2020) are the values of the equatorial coordinates of the objects (referred to epoch 2458838.92 JD or 10:4:48.00 UT on December 21, 2019 and 2458810.25 JD or 18:0:0.00 UT on November 22, 2019) and the geocentric distance (in the range 80–200 au). It is important to realize that due to parallax, the apparent position of these candidates will trace out an ellipse on the sky over the course of a year (Gaudi & Bloom 2005). Such a parallactic ellipse will have a maximum dimension of 17.′2 for a candidate located 200 au from the Sun and 21.′5 for the one at 160 au; the ellipse will have maximum eccentricity for those objects with very low values of the ecliptic latitude and it will be nearly circular for those close to the ecliptic pole. In addition to the apparent parallactic motion, the candidates will have a proper motion due to its intrinsic displacement as they go around the barycentre of the Solar system. When observing at quadrature, Earth's parallactic motion is close to zero; therefore, the observed rate of motion is the direct result of the object's orbital motion and can be estimated using Eq. (2). For a range in distance of 80–200 au, the proper motion values are in the range 30.′2 to 7.′6 per year, respectively, with 10.′7 per year for a distance of 160 au. Unless the true values of the relevant parameters of the candidates deviate significantly from those in table 2 of Rice & Laughlin (2020), the survey area size should have been sufficient to enable detections, particularly in the case of the most distant candidate.

The fields targeted by our proof-of-concept mini-survey were observed at relatively high airmasses (see Section 2). Therefore, it can be argued that our null result could be due to enhanced extinction caused by observing at such low elevations. However, this is likely not the case because the same EURONEAR collaboration carried out a nearly concurrent mini-survey looking for Atira and Vatira asteroids (see e.g. Greenstreet, Ngo & Gladman 2012) using the same instrumental setup and similar automated reduction pipeline. Atiras or Interior Earth Objects (IEOs) have aphelion distances <0.983 au and can only be observed at low solar elongations (often <70°); Vatiras have aphelia <0.718 au, are observed at very low solar elongations (typically <40°–45°), and just one such object is currently known (Bolin et al. 2020; de la Fuente Marcos & de la Fuente Marcos 2020; Greenstreet 2020), 594913 'Ayloi'chaxnim (2020 AV$_2$). Although the nearly concurrent EURONEAR small-scale survey (12 nights with an average time of 1.5 h per night devoted to searching for Vatira and Atira asteroids towards the evening and early morning skies) did not find any new Vatiras or IEOs, it did observe at elevations in the range 15°–30° and recovered known objects at apparent magnitudes close to or above 23 — for example 2017 HO$_{20}$, a main belt asteroid that was observed near conjunction. Furthermore, Fig. 2, top panel, shows the r'-magnitude distribution of the detected stars from one representative pointing out of the 77 (×5) pointings intended to recover the *TESS* candidate in Cepheus. The histogram was produced using the Matplotlib library (Hunter 2007) with sets of bins computed using NumPy (van der Walt, Colbert & Varoquaux 2011; Harris et al. 2020) by applying the Freedman and Diaconis rule (Freedman & Diaconis 1981). Figure 2, bottom panel, shows the expected S/N for *WHT* prime-focus imaging as a function of the exposure time from the exposure time calculator (ETC)[11] for a similar camera (Red+4, PFIP) for observations carried out under a seeing of 0.″9 at an airmass of 2.3 in dark time and R=23.2 mag. TNOs have color index $V-R$ in the range 0.2–1.2 (see e.g. Peixinho, Delsanti & Doressoundiram 2015). Consistently, we are confident that we reached a limiting magnitude r'=23.0 mag, which actually corresponds to V>23.0 mag (in fact, it could be 23.2–24.2 mag). Therefore, our distant TNO candidate survey could have detected candidates 9 and 11 in table 2 of Rice & Laughlin (2020) unless both candidates are much fainter than predicted or they are false positives in *TESS* data. In any case, Rice & Laughlin (2020) stated that many if not most of the high signal significances reported in their table 2 could be the result of unmodelled systematic errors. On the other hand, in the fields observed towards Cepheus, there are a few bright stars that might have hidden a putative moving object with the properties of candidate 9; we estimate that the probability of having missed the candidate as a result of it moving projected towards one of those bright stars is <1 per cent (considering the area affected by the bright stars and associated diffraction spikes).

5 SUMMARY AND CONCLUSIONS

We have performed, to our knowledge, the first ever search to recover outer Solar system body candidates found in data from NASA's *TESS* mission. We surveyed, in Sloan r', two areas of sky (square patches of over 1°×1°) around the circumpolar *TESS* candidates located at (07$^{\rm h}$:00$^{\rm m}$:15$^{\rm s}$, +86°:55′:19″), 202.8 au from Earth (candidate 9 in Rice & Laughlin 2020), and (06$^{\rm h}$:39$^{\rm m}$:47$^{\rm s}$, +83°:43′:54″) at 162.1 au (candidate 11), with the 4.2-m *WHT* and a QHY600L CMOS camera mounted on-axis at its prime focus. Our results are summarized as follows.

(i) We were unable to recover either of the candidates at Sloan r'⩽23 mag.
(ii) After considering both visibility and detectability issues we interpret our null detections as evidence that either both candidates are actually much fainter than predicted or that they are false positives in *TESS* data.

These findings emphasize the need for independent confirmation of detections of distant Solar system object candidates resulting from blind shift-and-stack searches.

ACKNOWLEDGEMENTS

We thank the referee for a constructive and useful report. This work was developed within the framework of the EURONEAR collaboration and it is based on observations made with the *William Herschel* Telescope (operated by the *Isaac Newton* Group of Telescopes, ING), proposals SW2021a24 and SW2021a10. We are thankful to the following ING staff who planned, carried out, and reported our service observations: Lara Monteagudo, Norberto Gonzalez, Yeisson Osorio, and Richard Ashley. CdlFM and RdlFM thank A. I. Gómez de Castro for providing access to computing facilities, and S. Deen and J. Higley for comments on TNOs.

[11] http://catserver.ing.iac.es/signal/index.php

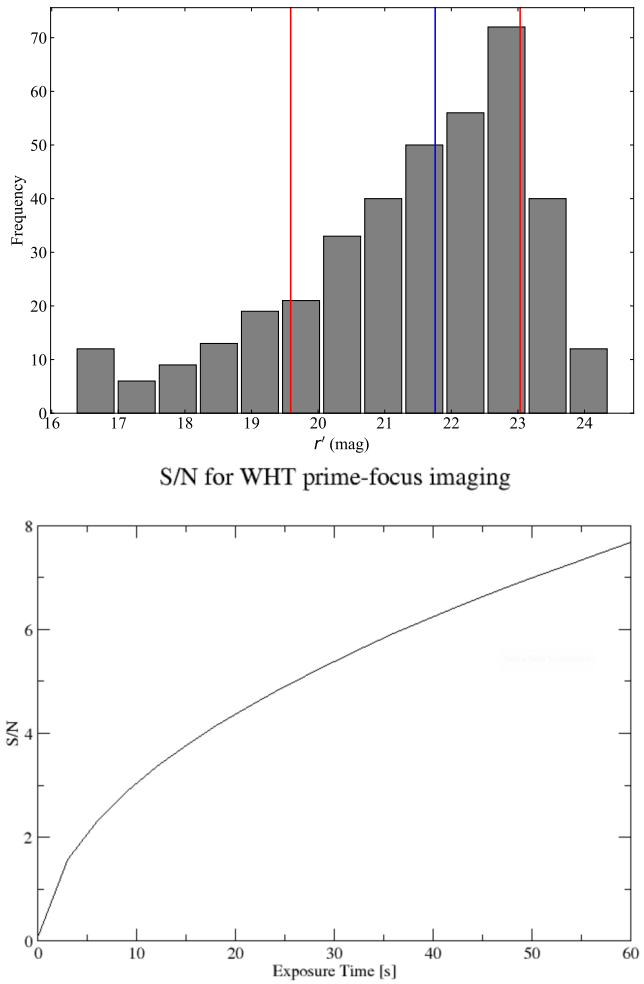

Figure 2. Completeness limit and S/N. The top panel shows the magnitude distribution of the stars detected from a representative pointing in Cepheus, observed at an elevation of 25° (using Pan-STARRS DR1 as a reference catalog, Flewelling et al. 2020). The median is shown in blue and the 16th and 84th percentiles are in red. In the histogram, bins were computed using the Freedman and Diaconis rule (Freedman & Diaconis 1981). The bottom panel displays the S/N for *WHT* prime-focus imaging as a function of the exposure time from the ETC of the Red+4 instrument with a seeing of 0.″9 at an airmass of 2.3 and R=23.2 mag. A S/N ratio close to 5.5 is expected to be reached for a 30 s integration.

This work was partially supported by the Spanish 'Ministerio de Economía y Competitividad' (MINECO) under grant ESP2017-87813-R and the 'Agencia Estatal de Investigación (Ministerio de Ciencia e Innovación)' under grant PID2020-116726RB-I00 /AEI/10.13039/501100011033. In preparation of this Letter, we made use of the NASA Astrophysics Data System and the MPC data server. This research has made use of SAOImage DS9, developed by the Smithsonian Astrophysical Observatory.

DATA AVAILABILITY

The data underlying this article will be shared on reasonable request to the corresponding author.

REFERENCES

Batygin K., Brown M. E., 2016, AJ, 151, 22
Becker J. C. et al., 2018, AJ, 156, 81
Bernstein G., Khushalani B., 2000, AJ, 120, 3323
Bertin E., 2006, in Gabriel C., Arviset C., Ponz D., Solano E., eds, ASP Conf. Ser. Vol. 351, Astronomical Data Analysis Software and Systems XV. Astron. Soc. Pac., San Francisco, p. 112
Bertin E., Arnouts S., 1996, A&AS, 117, 393
Bertin E., Mellier Y., Radovich M., Missonnier G., Didelon P., Morin B., 2002, in Bohlender D. A., Durand D., Handley T. H., eds, ASP Conf. Ser. Vol. 281, Astronomical Data Analysis Software and Systems XI. Astron. Soc. Pac., San Francisco, p. 228
Bolin B. T. et al., 2020, MPEC Circ., MPEC 2020-A99
de la Fuente Marcos C., de la Fuente Marcos R., 2014, MNRAS, 443, L59
de la Fuente Marcos C., de la Fuente Marcos R., 2018, Res. Notes AAS, 2, 167
de la Fuente Marcos C., de la Fuente Marcos R., 2020, MNRAS, 494, L6
de León J., de la Fuente Marcos C., de la Fuente Marcos R., 2017, MNRAS, 467, L66
Fitzsimmons A., 2000, in Fitzsimmons A., Jewitt D., West R. M., eds, Minor Bodies in the Outer Solar System. Springer, Berlin, Heidelberg, pp 87–98
Flewelling H. A. et al., 2020, ApJS, 251, 7
Freedman D., Diaconis P., 1981, Z. Wahrscheinlichkeitstheorie verw. Gebiete, 57, 453
Gaudi B. S., Bloom J. S., 2005, ApJ, 635, 711
Greenstreet S., 2020, MNRAS, 493, L129
Greenstreet S., Ngo H., Gladman B., 2012, Icarus, 217, 355
Harris C. R. et al., 2020, Nature, 585, 357
Hernandez S., Hankey M., Scott J., 2019, AAS Meeting Abstr., 233, 245.03
Holman M. J., Payne M. J., Pál A., 2019, Res. Notes AAS, 3, 160
Hunter J. D., 2007, CSE, 9, 90
Jewitt D., 1999, Annu. Rev. Earth Planet. Sci., 27, 287
Joye W. A., Mandel E., 2003, in Payne H. E., Jedrzejewski R. I., Hook R. N., eds, ASP Conf. Ser. Vol. 295, Astronomical Data Analysis Software and Systems XII. Astron. Soc. Pac., San Francisco, p. 489
McNeill A., Mommert M., Trilling D. E., Llama J., Skiff B., 2019, ApJS, 245, 29
Pál A., Molnár L., Kiss C., 2018, PASP, 130, 114503
Pál A. et al., 2020, ApJS, 247, 26
Payne M. J., Holman M. J., Pál A., 2019, Res. Notes AAS, 3, 172
Peixinho N., Delsanti A., Doressoundiram A., 2015, A&A, 577, A35
Raab H., 2012, ascl.soft. ascl:1203.012
Rice M., Laughlin G., 2020, PSJ, 1, 81
Ricker G. R. et al., 2015, JATIS, 1, 014003
Rudenko M., 2016, in Chesley S. R., Morbidelli A., Jedicke R., Farnocchia D., eds, Asteroids: New Observations, New Models. Proceedings of the International Astronomical Union, IAU Symposium, Vol. 318, Cambridge University Press, Cambridge, UK, pp 265–269
Sheppard S. S., Trujillo C. A., Oldroyd W. J., Tholen D. J., Williams G. V., 2018, MPEC Circ., MPEC 2018-Y14
Sheppard S. S., Tholen D. J., Trujillo C. A., 2021, MPEC Circ., MPEC 2021-C187
Stănescu M., 2020, ascl.soft. ascl:2008.006
Stănescu M., Văduvescu O., 2021, A&C, 35, 100453
Trujillo C. A., Sheppard S. S., 2014, Nature, 507, 471
van der Walt S., Colbert S. C., Varoquaux G., 2011, CSE, 13, 22
Van Rossum G., Drake F. L., 1995, Python tutorial. Centrum voor Wiskunde en Informatica Amsterdam, The Netherlands
Woods D. F. et al., 2021, PASP, 133, 014503

This paper has been typeset from a TEX/LATEX file prepared by the author.